Investigation of dislocation movement by nuclear-spin-relaxation experiments in the rotating frame

G. Hut and A. W. Sleeswyk
Laboratorium voor Fysische Metaalkunde, Materials Science Centre, University of Groningen, Groningen, The Netherlands

H. J. Hackelöer, H. Selbach, and O. Kanert
Institut für Physik der Universität Dortmund, Dortmund, Germany
(Received 6 October 1975)

Dislocations moving at various velocities in ^{23}NaCl and ^{87}RbCl single crystals were studied by means of the spin-locking technique. The resulting spin-lattice relaxation time in the rotating frame $T_{1\rho}$ is strongly dependent on the plastic-deformation rate $\dot{\epsilon}$ and the quadrupole moments of the spins considered. The experimental results are in accord with a theoretical expression for $T_{1\rho}$ based on an adaption of the relaxation model of Rowland and Fradin for atomic diffusion. Application of this theory leads to a "mean free path" of a moving dislocation which is determined by the distance between the forest dislocations; this agrees with the value obtained for the strain-rate sensitivity. The range of validity of the adapted Rowland and Fradin model is discussed.

I. INTRODUCTION

During plastic deformation of crystalline solids dislocation motions of various kinds may occur[1]; this depends for any material on external parameters such as strain rate and temperature. In what follows thermally activated dislocation motion is regarded as a glide process in which a dislocation under stress can overcome obstacles with the aid of thermal fluctuations of the lattice.

A long-standing problem in this field is the connection between the macroscopic strain rate and the density and average velocity of moving dislocations. Orowan gave the following equation[2] linking these properties:

$$\dot{\epsilon} = \phi b \rho_m v, \tag{1}$$

with ϕ geometry factor ($\approx \frac{1}{2}$), b is the magnitude of the Burgers vector, ρ_m is the mobile-dislocation density, and v is the mean dislocation velocity. For a given strain rate the product $\rho_m v$ must be a constant. Unknown, however, is the fraction of the total dislocation density which is mobile and the time scale factor of the atomic movements caused by the dislocation motion. Application of values for dislocation velocities near the free surface as obtained from stress pulse-etchpit experiments[3] to tests at constant strain rates of the bulk material raises doubt because of the very different experimental conditions.

Because the process of dislocation motion is made up of atomic movements nuclear-magnetic-resonance techniques should offer a possiblity to determine the way in which the dislocation progresses through the crystal as a function of time utilizing nuclear spin relaxation as a tool. Experiments of this type cover very large time intervals: from 10^{-8} sec(T_1) via 10^{-4} sec(T_2) to 10^{2} sec(T_{1D}), which allows scanning the velocity region.

In doing this we found[4-6] that the atomic movements involved are in the ultraslow-motion region where T_1 and T_2 are constant and where T_{1D} is a function of these movements. The theory which was originally given by Slichter and Ailion[7] and by Rowland and Fradin[8] for self-diffusion, could be adapted to dislocation movement; in what follows this modified theory will be referred under the acronym SARF.

II. THEORY

A. Dynamic dislocation problem

The dislocation motion in alkalihalogenide single crystals during compression in the ⟨100⟩ direction is studied. In the stress-strain curve four regions can be distinguished (Fig. 1): A region of "pre-yield" up to a plastic strain of approximately 0.1%. It is observed by Pratt,[9] Mendelson,[10] and Heidemann[12] that plastic deformation in this region is connected to slip on the four equivalent ⟨110⟩{110}-slip systems with the same Schmidt factor.

Stage I, a region of low constant work-hardening rate. The deformation in stage I is dominated by slip on only one of the four slip systems active during pre-yield (Davidge and Pratt,[13] Hesse,[11] Argon *et al.*,[14] Hesse and Hobbs,[15] Hesse and Matucha,[16] and Heidemann[12]). In this region the increase of the shear strain takes place by the broadening of the slip planes into bands and by an increase in the number of bands[11-13]: the deformation in stage I is due to the activation of dislo-

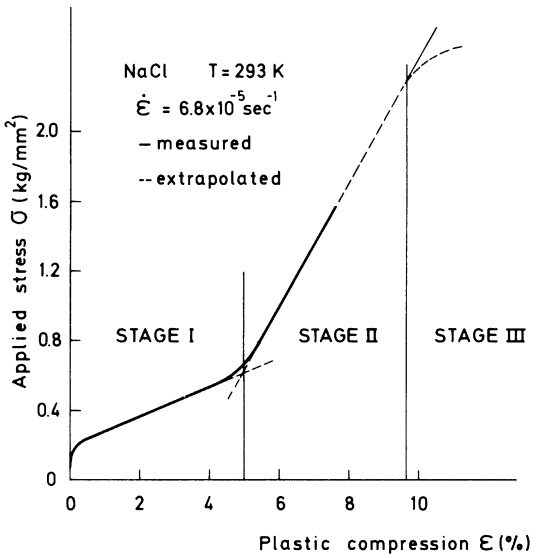

FIG. 1. Schematic stress-strain curve of a NaCl single crystal. Our own measurements were confined to regions I and II.

cations on new slip planes whereas a further dislocation movement in the existing slip planes is impeded by obstacles. Stage I is terminated when the distance between the dislocations in the slip planes approaches the distance—~1.2 μm—between the slip bands. Subsequently, polygonization sets in.[12,13]

Stage II, a region with a high constant work-hardening rate. The deformation is dominated by slip on the same slip system active in stage I,[12,13,16] although it is found that a small amount of slip on secondary systems takes place as was found by Matucha,[17] Heidemann,[12] and Davidge and Pratt.[13]

Stage III, at large strains, shows a decreasing work-hardening rate. Cross slip of screw dislocations can explain in this region the behavior of the stress-strain curve as a function of strain rate and temperature. In our experiments the strains did not go beyond stage II.

During a deformation test the total dislocation density increases: in general it is found (Matucha *et al.*[18] and Hesse and Hobbs[15]) that in alkalihalogenide single crystals in stages I and II, just as in fcc metals, the square root of the dislocation density ρ is proportional to the shear stress σ that has been reached:

$$\sigma = \alpha G b \sqrt{\rho}, \tag{2}$$

where α is a constant of the material, G is the shear modulus, and b is the Burgers vector. Typical values of ρ are 10^4 dislocations/cm^2 (before deformation) and $\rho = 10^8$ dislocations/cm^2 (after about 10% plastic deformation).

Dislocations of the edge type prevail in the crystals considered: Hesse[11] found in ⟨100⟩-orientated NaCl crystals an edge-screw dislocation density ratio of ~3 in the stages I and II; Davidge and Pratt[13] found for the same ratio the value ~5. From the obstacle model of thermally activated dislocation motion[1] which has been worked out in detail by computer simulation (Foreman and Makin[19]), it is probable that dislocation motion is discontinuous. The waiting time τ at an obstacle of a dislocation under stress may be assumed to be much longer than the time τ_s it actually moves to the next obstacle or stable position. The rapid movement of a dislocation between obstacles is called a jump. The mean velocity of a dislocation is then determined by τ and the swept-out distance nb expressed as an integer n times the Burgers vector b of the dislocation. The maximum value of τ_s is determined by the velocity of a shear wave in the crystal.

B. Relaxation theory

If the rotating frame is exactly at resonance (Abragam[20] and Farrar and Becker[21]), the governing truncated nuclear spin Hamiltonian is given by

$$\hat{H} = \hat{H}_D + \hat{H}_Q, \tag{3}$$

where $\hat{H}_D$ and $\hat{H}_Q$ are the secular parts of the dipolar and quadrupolar Hamiltonians, respectively. From this and the spin temperature concept together with the law of energy conservation the Slichter-Ailion-Rowland-Fradin formula[7,8] (SARF) for the relaxation rate $1/T_1 = R_D^{(\rho)}$ for the resonant spins of the specimen in the rotating frame due to ultraslow atomic motions is obtained:

$$R_D^{(\rho)} = G_D \frac{\langle \omega_D^2 \rangle}{\gamma^2 H_1^2 + \langle \omega_D^2 \rangle + \langle \omega_Q^2 \rangle} \frac{1}{\tau} + G_Q \frac{\langle \omega_Q^2 \rangle}{\gamma^2 H_1^2 + \langle \omega_D^2 \rangle + \langle \omega_Q^2 \rangle} \frac{1}{\tau}. \tag{4}$$

Here G_D and G_Q are the dipolar and quadrupolar geometry factors, respectively, γ is the gyromagnetic ratio of the spins considered, H_1 is the strength of the locking field, $\langle \omega_D^2 \rangle$ is the mean dipolar energy, $\langle \omega_Q^2 \rangle$ is the mean quadrupolar energy determined only by the lattice defects in the cubic system, and τ is the mean waiting time between jumps.

The validity of Eq. (4) is subject to the following conditions:

(a) $\tau \gg \omega_D^{-1}$, where ω_D is the dipolar line width. In this case the nonsecular part of the dipolar Hamiltonian will exchange energy by flip-flop transitions between the nuclear spins in times short compared to the waiting time τ. The cross relaxation within the spin system is very

rapid, consequently the spin system can be characterized by a common spin temperature prior to each dislocation jump (validity of the spin temperature concept[7]),

(b) $\langle\omega_Q^2\rangle^{1/2} \lesssim \langle\omega_D^2\rangle^{1/2}$; for nuclei with spin $I>\frac{1}{2}$, the requirement (a) of rapid transfer of energy between the spins necessitates that $\langle\omega_Q^2\rangle^{1/2} \lesssim \langle\omega_D^2\rangle^{1/2}$. If so, the cross-relaxation process given by the magnetic dipole-dipole interaction is unaffected by the quadrupole effects. A quadrupole interaction with $\langle\omega_Q^2\rangle^{1/2} \gg \langle\omega_D^2\rangle^{1/2}$, will change the spacings of the nuclear spin levels markedly and thus eliminate many of the resonances between neighboring spins which are needed for cross relaxation. Condition (b) extends the uniform spin temperature concept to nuclei with $I>\frac{1}{2}$. In practice the condition is only valid for spins with a moderate quadrupole moment and for cubic lattices.[8]

(c) $\tau_S \ll \omega_0^{-1}$, where ω_0 is the Larmor frequency of the spins considered. The time the dislocation spends in the actual process of jumping is then short compared to the precession period of the nuclei involved with the jump so that the spin orientation is the same immediately after the jump as it was immediately before the jump. In the density-matrix approach, the assumption is equivalent to stating that the spin density matrix does not change during the actual jumping process, or that the "sudden" approximation of quantum mechanics can be applied to the jumping process.[7]

Analogous to the way in which G_Q and G_D of Eq. (4) were derived for self-diffusion it is possible to do this for a spin system of which the positions of the spins are influenced by moving dislocations. Consider a specimen of volume V containing N resonant nuclei. At the moment $t=0$ the total dislocation density is ρ dislocations/cm^2. At the moment $t=\tau$ a mobile fraction ρ_m has moved. A sessile fraction ρ_S, mainly forest dislocations with unaltered positions, is given by

$$\rho = \rho_S + \rho_m. \tag{5}$$

In order to calculate G_Q one has to determine the quadrupole Hamiltonian of all spins before and after the motion of the dislocations. Suppose a nucleus i experiences an electric field gradient B_{ik} from a surrounding nucleus k. The total electric field gradient B_i at site i due to all nuclei of the specimen is then

$$B_i = \sum_{k=1}^{N} B_{ik}, \tag{6}$$

and the quadrupole Hamiltonian of the system at $t=0$ is then equal to

$$\hat{H}_Q = \sum_{i=1}^{N}\sum_{k=1}^{N} B_{ik}\hat{Q}(\hat{I}_i), \tag{7}$$

with $\hat{Q}(\hat{I}_i) = 3\hat{I}_{zi}^2 - \hat{I}^2$, $\hat{I}$ being the spin operator.

Let $\hat{H}_Q'$ be the quadrupole Hamiltonian at the time τ, G_Q is then defined[8] as

$$G_Q = (\hat{H}_Q^2 - \hat{H}_Q\hat{H}_Q')/\hat{H}_Q^2. \tag{8}$$

Using condition (b) of Eq. (4), i.e., the "sudden" approximation, in which the spin-dependent part of (7) remains a constant, Eq. (8) becomes

$$G_Q = \frac{\sum_{i=1}^{N}\sum_{k=1}^{N} B_{ik}^2 - \sum_{i=1}^{N}\sum_{k=1}^{N} B_{ik}B_{ik}'}{\sum_{i=1}^{N}\sum_{k=1}^{N} B_{ik}^2}. \tag{9}$$

As not all the nuclei contribute to the field gradient, the summation can be restricted to the n surrounding nuclei which do contribute:

$$\sum_{i=1}^{N}\sum_{k=1}^{N} B_{ik}^2 = \sum_{i=1}^{N}\sum_{k=1}^{n} B_{ik}^2. \tag{10}$$

Supposing that N_ρ nuclei are perturbed by dislocations and remembering that $B_i \equiv 0$ in the case of an ideal cubic lattice, the denominator of Eq. (9) can be written

$$\sum_{i=1}^{N}\sum_{k=1}^{n} B_{ik}^2 = (N-N_\rho)\sum_{k=1}^{n} B_k^2 + \sum_{i=1}^{N_\rho}\sum_{k=1}^{n} B_{ik}^2 = \sum_{i=1}^{N_\rho}\sum_{k=1}^{n} B_{ik}^2. \tag{11}$$

If n_ρ is the number of nuclei per cm dislocation length in a cylinder within a certain radius, coaxial to the dislocation line and V is the volume of the sample, then the expression

$$N_\rho = \rho V n_\rho \tag{12}$$

is valid. Combination of Eqs. (10)–(12) results in

$$\sum_{i=1}^{N}\sum_{k=1}^{N} B_{ik}^2 = \rho V \sum_{i=1}^{n_\rho}\sum_{k=1}^{n} B_{ik}^2. \tag{13}$$

The numerator of Eq.(9) can be treated in a similar manner: The summation is again split up in one over perturbed and one over unperturbed nuclei which results in

$$\sum_{i=1}^{N}\sum_{k=1}^{N} B_{ik}B_{ik}' = (N-N_\rho)\sum_{k=1}^{n} B_k^2 + \sum_{i=1}^{N_\rho}\sum_{k=1}^{n} B_{ik}B_{ik}' = \sum_{i=1}^{N_\rho}\sum_{k=1}^{n} B_{ik}B_{ik}'. \tag{14}$$

Dividing the number of perturbed nuclei in a fraction perturbed by sessile and a fraction perturbed by mobile dislocations at the time $t=\tau$ according to

$$N_{\rho_s}=\rho_s V n_\rho \tag{15}$$

and

$$N_{\rho_m}=\rho_m V n_{\rho_m} \tag{16}$$

(n_{ρ_m} is the number of nuclei per cm dislocation length involved in a dislocation jump of length nb), Eq. (14) can be developed as

$$\sum_{i=1}^{N_\rho}\sum_{k=1}^{n} B_{ik}B_{ik}' = \rho_s V\sum_{i=1}^{n_\rho}\sum_{k=1}^{n} B_{ik}^2 + \rho_m V\sum_{i=1}^{n_{\rho_m}}\sum_{k=1}^{n} B_{ik}B_{ik}'. \tag{17}$$

Combining Eqs. (5), (10), (13), and (17) yields

$$\begin{aligned} G_Q &= 1-\left(\sum_{i=1}^{N}\sum_{k=1}^{N} B_{ik}B_{ik}'\right)\Big/\sum_{i=1}^{N}\sum_{k=1}^{N} B_{ik}^2 \\ &= 1-\left(\rho V\sum_{i=1}^{n_\rho}\sum_{k=1}^{n} B_{ik}^2\right)\Big/\rho V\sum_{i=1}^{n_\rho}\sum_{k=1}^{n} B_{ik}^2 - \rho_m V\left(\sum_{i=1}^{n_{\rho_m}}\sum_{k=1}^{n} B_{ik}B_{ik}' - \sum_{i=1}^{n_\rho}\sum_{k=1}^{n} B_{ik}^2\right)\Big/\rho V\sum_{i=1}^{n_\rho}\sum_{k=1}^{n} B_{ik}^2 \\ &= G_Q = \frac{\rho_m}{\rho}\left[1-\left(\sum_{i=1}^{n_{\rho_m}}\sum_{k=1}^{n} B_{ik}B_{ik}'\right)\Big/\sum_{i=1}^{n_\rho}\sum_{k=1}^{n} B_{ik}^2\right] = \frac{\rho_m}{\rho}\, g_Q. \end{aligned} \tag{18}$$

G_D can be calculated in an analogous way: starting from the dipolar Hamiltonian of the spin system at $t=0$:

$$\hat{H}_D = \sum_{i<k}^{N}\sum_{k=1}^{N} A_{ik}\hat{D}(\hat{I}_{ik}), \tag{19}$$

where $\hat{D}(\hat{I}_{ik}) = 3\hat{I}_{zi}\hat{I}_{zk} - \hat{I}_i\hat{I}_k$ and A_{ik} is the geometrical part of the dipolar Hamiltonian.[7] H_D' being the dipolar Hamiltonian at time $t=\tau$, G_D is then defined as

$$G_D = (\hat{H}_D^2 - \hat{H}_D\hat{H}_D')/\hat{H}_D^2. \tag{20}$$

Using again the sudden approximation Eq. (20) can be written

$$G_D = \frac{\sum_{i<k}^{N}\sum_{k=1}^{N} A_{ik}^2 - \sum_{i<k}^{N}\sum_{k=1}^{N} A_{ik}A_{ik}'}{\sum_{i<k}^{N}\sum_{k=1}^{N} A_{ik}^2}. \tag{21}$$

The further calculation is quite similar to that of G_Q; there is however one important difference: The dipolar Hamiltonian does not vanish far from a dislocation like the quadrupole Hamiltonian. Therefore the summation should be over all atoms. The resulting expression is

$$\begin{aligned} G_D &= \frac{\rho_m n_\rho}{n_0}\left[1-\left(\sum_{i<k}^{n_{\rho_m}}\sum_{k=1}^{n_c} A_{ik}A_{ik}'\right)\Big/\sum_{i<k}^{n}\sum_{k=1}^{n_c} A_{ik}^2\right] \\ &= \frac{\rho_m n_\rho}{n_0}\, g_D, \end{aligned} \tag{22}$$

with n_0 the number of spins per cm^3, n_c the number of spins contributing to A_{ik}, g_D the dipolar geometry factor for 1-cm dislocation length. Assuming that g_D is of the same order as g_Q, a rough estimate gives then $G_D/G_Q \approx (n_\rho/n_0)\rho$. On the basis of some realistic values, e.g., $n_\rho \approx 10^9$ cm^{-1}, $\rho \approx 10^8$ cm^{-2}, $n_0 \approx 10^{21}$ cm^{-3} it follows that $G_D \ll G_Q$. The latter is confirmed experimentally.[5]

The SARF formula (4) reduces then for moving dislocations to

$$R_D^{(\rho)} = \frac{\langle\omega_Q^2\rangle}{\gamma^2H_1^2 + \langle\omega_D^2\rangle + \langle\omega_Q^2\rangle}\,\frac{\rho_m}{\rho}\, g_Q\,\frac{1}{\tau}. \tag{23}$$

Combining the Orowan equation (1), the expression for the mean dislocation velocity $v = nb/\tau$ and Eq. (23),

$$R_D^{(\rho)} = \frac{\langle\omega_Q^2\rangle}{\gamma^2H_1^2 + \langle\omega_D^2\rangle + \langle\omega_Q^2\rangle}\,\frac{1}{\rho}\,\frac{1}{\phi b^2}\,\frac{g_Q}{n}\,\dot{\epsilon}, \tag{24}$$

is obtained.

Assuming a statistical distribution of dislocations one may write (Kanert and Mehring[22])

$$\langle\omega_Q^2\rangle = A\rho, \tag{25}$$

with $A = \text{const}(\approx 0.13$ cm^2 sec^{-2} for ^{23}NaCl) (Baumhoer *et al.*[23]), Eq. (24) can then be rewritten

$$R_D^{(\rho)} = \frac{A}{\gamma^2H_1^2 + \langle\omega_D^2\rangle + \langle\omega_Q^2\rangle}\,\frac{1}{\phi b^2}\,\frac{g_Q}{n}\,\dot{\epsilon}. \tag{26}$$

To calculate the value of g_Q one should evaluate the field gradients of Eq. (5). This, however, is a tedious task for atoms around a dislocation because of the slow convergence of the summation: Such calculations have been carried out only for perfect crystals using their symmetry properties

(De Wette[24] and De Wette and Schacher[25]). To avoid this difficulty we used for our calculation of g_Q the approximation[22]

$$B_i = \sum_{k=1}^{N} B_{ik} = B_0 \Gamma(\theta_i, \alpha_v) f(r_i), \tag{27}$$

which is valid in cubic lattices for field gradients caused by dislocations. Here B_0 is a constant for the material and type of dislocation[22] (screw or edge) considered. The function $f(r_i)$ depends on the distance r_i between the nucleus i and the dislocation line, whereas Γ is the angular function determined by the type of dislocation, by the angle θ_i between the vector $\vec{r}_i$ and the slip direction, and by $\alpha_v = \cos(H_0, X_v)$ (X_v is the cube axis of the dislocation frame; $v = 1, 2, 3$).

Two possibilities can be distinguished:

(a) $r_i > r_c$, where r_c is a critical radius indicating the range above which the displacements of the nuclei due to the dislocation can be calculated adequately from linear elasticity theory. In ionic crystals the value $r_c \approx 3b$ (recall b is the magnitude of the Burgers vector) is usually valid. In the region where $r_i > r_c$, the expression

$$f(r_i) = 1/r_i \tag{28}$$

may be applied, and the electric field gradient is then given by

$$B_i = B_0 \Gamma(\theta_i, \alpha_v) r_i^{-1}. \tag{29}$$

The value of $B_0\Gamma$ is only slightly dependent on the character, i.e., edge or screw, of the dislocation.[22]

(b) $r_i \leq r_c$. In this range, within the core of the dislocation, Eq. (28) breaks down. To avoid the difficulties mentioned before we used again an approximation.

Granzer *et al.*[26] calculated the positions of atoms in the core of an edge dislocation in NaCl. They used anisotropic boundary conditions at the core radius and allowed the atoms inside the core to relax to their final positions. This was done for several potentials [in their article appeared a printing error in Eq. (2): the denominator of the arctan function in the expression for $u(x, y)$ should be $x + y\cos\alpha$ instead of $x + y\sin\alpha$] at the core radius and allowed the atoms inside the core to relax to their final positions. This was done for several potentials. From their calculation of the energy per atomic plane they found a deviation from the well-known $1/r$ behavior for three points inside the core.

Using the same principles under which Eq. (28) was derived we assumed that the field gradient in the core could be approximated by fitting a parabola through these three points, having its axis at $r_i = 0$ and the same value and slope at $r_i = r_c$ as the field gradient function B_i given by Eq. (29). For the core atoms, i.e., $r_i \leq r_c$, we found in this way the distance function $f(r_i)$ of the electric field gradient

$$f(r_i) = -\tfrac{1}{54} r_i^2 + 0.5, \tag{30}$$

where the unit of r_i is the Burgers vector. Assuming no change in the angular function Γ going from $r > r_c$ to $r < r_c$ the calculation of g_Q reduces to

$$g_Q = 1 - \frac{\sum_{i=1}^{n_p} \Gamma(\theta_i, \alpha_v) f(r_i) \Gamma(\theta_i', \alpha_v') f(r_i')}{\sum_{i=1}^{n_p} \Gamma^2(\theta_i, \alpha_v) f^2(r_i)}, \tag{31}$$

where $B_i' = B_0 \Gamma(\theta_i', \alpha_v') f(r_i')$ the field gradient at site i after the sudden motion of the dislocation across a free path (see Fig. 2).

We calculated g_Q for a free path trajectory of an edge dislocation across n Burgers vectors, n being an integer. Assuming that the configuration of the dislocation line before and after the movement remains unchanged relative to the slip plane, i.e., relative to the external field H_0, it follows that $\alpha_v = \alpha_v'$. In this case the function Γ remains approximately constant, too. The computer program now was organized as follows (Fig. 2):

(a) A $[110](1\bar{1}0)$-edge dislocation is placed in the origin of a Cartesian frame.

(b) Using the corrected anisotropic displacement formula of Granzer *et al.*,[26] the position was calculated of an atom i in a rectangle with coordinates $(-X_{max}, X_{max} + n)$ and $(Y_{max}, -Y_{max})$ and outside a "core" square with sides determined by the x and y positions (−3 Burgers vectors, +3 Burgers vectors) and $(+3b, -3b)$.

(c) In the core square the position of atom i was taken from Granzer *et al.* from the calculation in which they used the Born-Mayer-Huggins potential. (The atomic positions they obtained are not very sensitive to the potential used.)

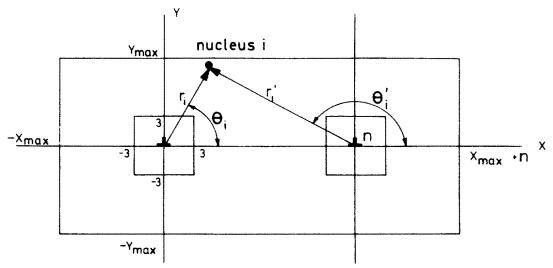

FIG. 2. Geometry of the variables used in the calculation of quadrupolar geometry factor g_Q for a mobile dislocation according to Eq. (31). The unprimed coordinates describe the initial position of the dislocation relative to the considered nucleus i, whereas the primed coordinates give the final position after a jump of the dislocation of step width n. The limiting values X_{max}, Y_{max} are determined by the convergence of the sums in Eq. (31).

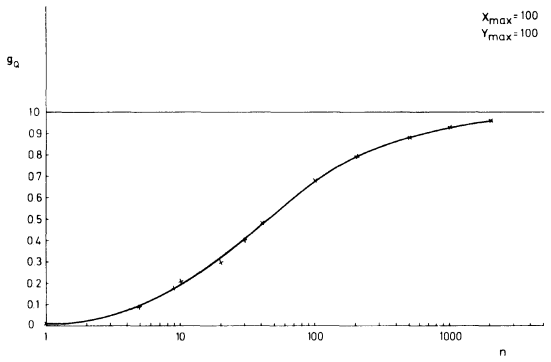

FIG. 3. Quadrupolar geometry factor g_Q for a mobile dislocation as a function of the step width n (in units of the Burgers vector b). As expected from the general formula (18), g_Q varies from zero (step width n equal zero, i.e, the unprimed and primed positions are identical) to one (step width equals infinity, i.e., no correlation between the unprimed and primed position).

(d) The field gradient was calculated using Eqs. (29) for (b) and (30) for (c).

(e) The dislocation is then allowed to move n Burgers vectors.

(f) The procedures (b)–(d) were repeated in order to calculate the field gradient of atom i after the movement.

(g) The procedures (b)–(f) were repeated for all atoms inside the large rectangle. From this g_Q [Eq. (31)] could be calculated.

The calculation was performed on the Cyber 74 computer of the University of Groningen. The parameters X_{max} and Y_{max} were varied over several orders of magnitude to determine g_Q as a function of n. The maximum number of atoms used for the calculation was 1 250 000. From this study it could be deduced that the convergence of g_Q for varying X_{max} and Y_{max} was rather good for values of $X_{max} = Y_{max} = 100$ Burgers vectors. Doubling of X_{max} and Y_{max} from these values changed g_Q with less than 1%. As an example the result of such a calculation is presented in Fig. 3.

For edge dislocations the core structures are known, and mainly for this reason we based the calculation of the geometry factor g_Q on the assumption that the dislocations were all of this type. We observed that for large step widths of edge dislocations g_Q becomes quite independent on detailed atomic positions in the core or elsewhere, and we have reason to suspect, therefore, that there would not be much of a difference between the effect of an edge or a screw dislocation.

III. EXPERIMENTAL DETAILS

The reported measurements were performed on ^{23}NaCl and ^{87}RbCl single high-purity crystals furnished by Kort Co. at Kiel (Germany). They were cleaved along {100} planes and then carefully polished to square prisms with the ⟨100⟩ direction as an axis and {100} and {110} side planes. After polishing the crystals were kept at 150 °C for at least 6 h and slowly cooled in air. The final dimensions were length, 25 mm, and width between side planes, 10.5 mm. After the deformation some randomly chosen crystals were investigated for their impurity content by means of a Perkin Elmer spectrophotometer. The concentrations of impurities, mostly Ca and K, were below 10 ppm. ^{23}Na and ^{87}Rb nuclei were chosen for investigation, because for these $\langle\omega_Q^2\rangle_{max} \lesssim \langle\omega_D^2\rangle$ (as will be shown afterward). One condition for the application of the SARF equation (4) is thus fulfilled. The spectrometer used is a commercial Bruker SXP 4-60 pulse spectrometer with a modified resonance circuit described elsewhere.[27] The decay signals obtained exhibited a signal to noise ratio of about 200 : 1 and were stored on a fast transient recorder (Biomation 802) and then transcribed on magnetic tape. Further processing of the decay signals was carried out by an on-line Varian 620/L computer.

The coil was mounted in a tensile machine, partly shown in Fig. 4. The inner rod (brass) can be displaced relative to the outer ones with a constant velocity. The distance between the rods was fixed by diaphragms with a large stiffness perpendicular to the rods axis and a low stiffness in the displacement direction. The diaphragms prevented the bars from buckling, which was effective up to a load of 200 kg: The maximum load in the experiments did not exceed this value. The cross head templates were manufactured from polyvinylchloride, so as to avoid bringing metal in the coil during a test. The cross head velocity could be stepwise varied from 10^{-5}, 3×10^{-5} cm/min, etc.,

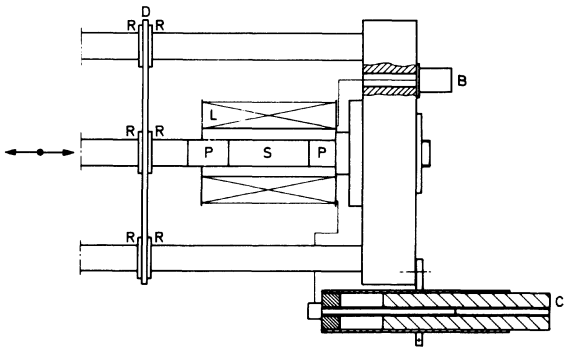

FIG. 4. Part of the mechanical tester which is inserted between the pole pieces and the probe head. D is the diaphragm, L is the coil, B is the connector to the spectrometer, S is the specimen, P is the PVC templates, and C is the condenser.

up to 1 cm/min. No plastic deformation in the machine itself took place. The direction of compressive deformation lies always in the ⟨100⟩ direction of the sample, perpendicular to the external field $\vec{H}_0$. The stress was measured by a strain-gauge load cell and the elongation by an inductive displacement transducer. Measurements at temperatures lower than room temperature were carried out by using a hollow polyvinylchloride cylinder around the coil as a cryostat, and blowing N_2 vapor through it or filling it with liquid N_2. The part of the tensile machine shown was placed in the gap of a 10-in. Bruker BE-25 magnet with a current stabilizer and an external Bruker NMR stabilizer B-SN 15.

IV. PRINCIPLE OF MEASUREMENTS

We oriented the crystals with one of the ⟨110⟩ directions parallel to the large external field $\vec{H}_0$ so as to avoid a possible orientation effect. In this case, the dislocation lines and the slip direction of the one activated set of the two possible conjugated ⟨110⟩ {110} slip systems will be equivalent to the other one. It will not make any difference then whether the number of moving dislocations in one set is larger than the other one.

An example of a typical measurement is shown in Fig. 5. From this it is apparent that an applied plastic strain rate $\dot{\epsilon} = (d/dt)(dL/L)$ causes a significant change in the relaxation time $T_{1\rho}$. In accordance with earlier observations (Hut *et al.*[4]) it was observed that the line shape and the exponential character of the decay are not affected by the plastic deformation rate. In Fig. 6 an example of a typical series of measurements is given.

From these results and from the exponential decay the dynamic part of the relaxation rate, $R_D^{(\rho)}$ can be calculated according to the expression

$$R_D^{(\rho)} = (1/T_{1\rho})_{\text{dyn.}} = (1/T_{1\rho})_{\dot{\epsilon}\neq 0} - (1/T_{1\rho})_{\dot{\epsilon}=0}. \qquad (32)$$

In doing this we found no dependence on temperature of $R_D^{(\rho)}$ in the region[4] 77–293 K and no dependence on the deformation ϵ.

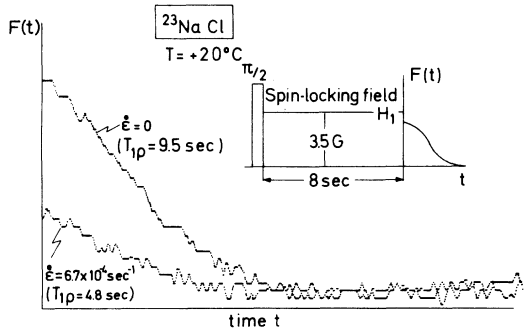

FIG. 5. Experimental result showing two free induction decays $F(t)$ after a spin locking sequence of 8 sec and a locking field H_1 of 3.5 G (see insert) with zero and finite plastic deformation rates $\dot{\epsilon}$. The values of $T_{1\rho}$ given in the figure are calculated from the usual expression $\hat{F}(\tau) = \hat{F}(0)\exp(-\tau/T_{1\rho})$ in which $\hat{F}$ is the maximum of $F(t)$.

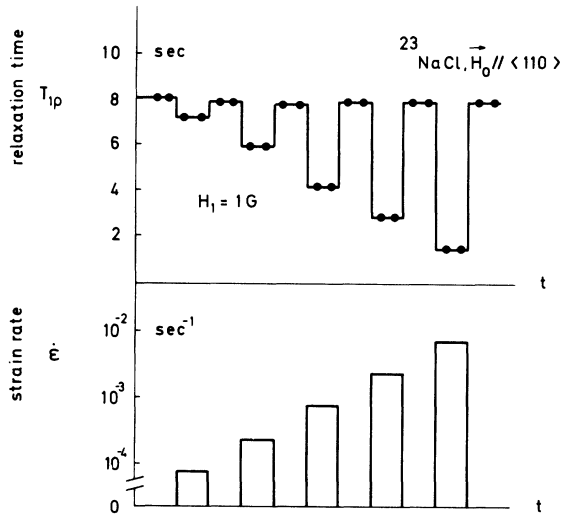

FIG. 6. Experimental run consisting of consecutive compressive deformations at increasing strain rate. The associated decrease in the total relaxation time $T_{1\rho}$ of ^{23}NaCl is shown in the upper half of the diagram. The variation in the relaxation time $T_{1\rho}$ follows that of the strain rate without any measurable time lag.

V. EXPERIMENTAL RESULTS AND EVALUATION

In order to check the conditions for the application of the SARF theory we measured for ^{23}NaCl as well as for ^{87}RbCl T_1 and T_2 during plastic deformation. T_1 was measured after a 180°-τ-90° pulse sequence: no change in signal height or line shape was observed with respect to the nondeforming case. From this we concluded that T_1 and T_2 are constant during plastic deformation in accordance with the conditions (b) and (a) required for Eq. (4).

In order to obtain experimental proof for a SARF-type equation for the dislocation motion, we measured $R_D^{(\rho)}$ as a function of $\dot{\epsilon}$ with H_1 as a parameter (Fig. 7). The slope of the curves up to $\dot{\epsilon} \approx 2\times 10^{-3}$ sec^{-1} is about 1 as predicted by Eq. (26). The small deviation from the straight lines at high deformation rates $\dot{\epsilon}$ in Fig. 7 are not completely clear. Estimates give that the deviations do not indicate the beginning of the usual maximum in the relaxation rate. We suspect that the available stiffness of the mechanical device, which is not well known, will produce in the high-velocity region lower deformation rates $\dot{\epsilon}$ in the sample

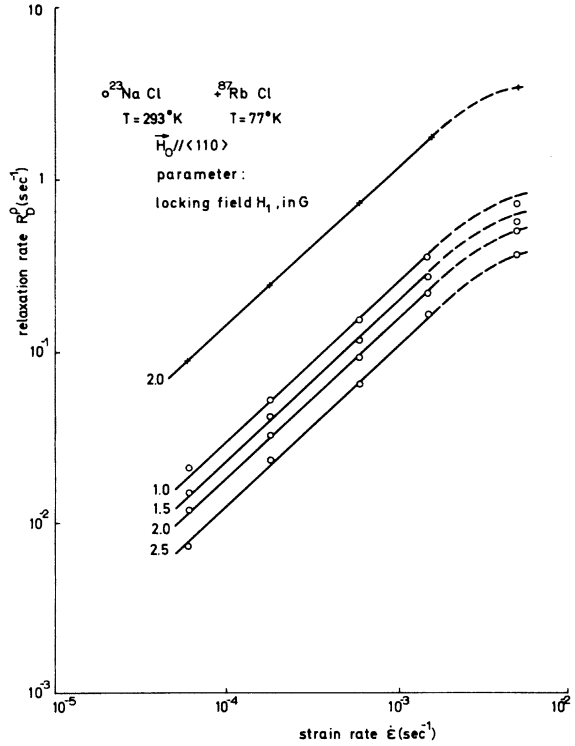

FIG. 7. Measured data of the dynamic part of the relaxation rate $R_D^{(\rho)}$ of ^{23}Na and ^{87}Rb as a function of the strain rate $\dot{\epsilon}$. The slope of the straight lines in the figure is in agreement with the theoretical relation (26).

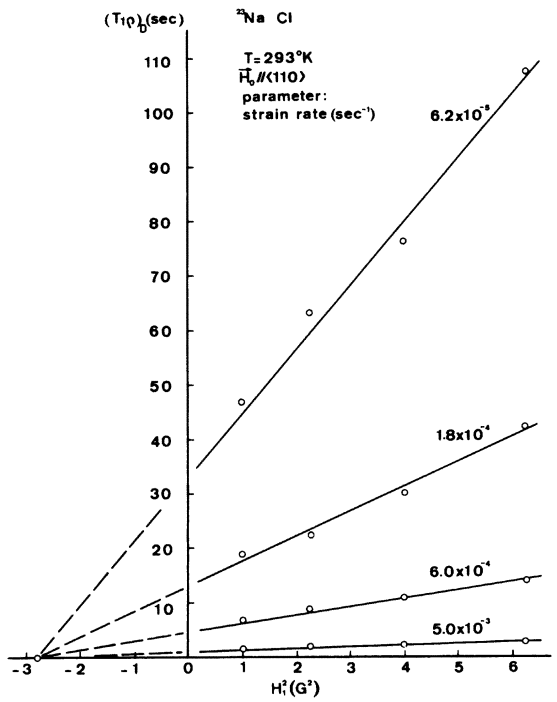

FIG. 8. Dynamic part of the relaxation time $(T_{1\rho})_D = (R_D{}^{\rho})^{-1}$ of ^{23}Na in NaCl vs the square of the locking field H_1 showing the linear relationship between $(R_D{}^{\rho})^{-1}$ and $H_1{}^2$ according to Eq. (26). The intersection of the lines with the abscissa is approximately in one point given by 2.8 G^2.

as would result from calculations using the known machine parameters. Thus, the plots of Fig. 7 justify application of a SARF-type formula. According to Eq. (26) a plot of the relaxation time $(T_{1\rho})_D = (R_D^{\rho})^{-1}$ vs H_1^2 will yield a straight line, which can be extrapolated to the intercept at $H_1^2 = -(1/\gamma^2)(\langle\omega_D^2\rangle + \langle\omega_Q^2\rangle)$. The slope of the line is determined by $C\dot{\epsilon}^{-1}$, with $C = \phi b^2 n/Ag_Q \simeq$ const. Figure 8 shows the results of such an evaluation of the experimental data confirming the theoretical prediction given by Eq. (26). The occurence of an apparent common point of intersection of the different experimental curves with the H_1^2 axis is explained by the fact that the change in $\langle\omega_Q^2\rangle$ with strain in the different samples yielding the data in Fig. 8 is small compared to $\langle\omega_D^2\rangle + \langle\omega_Q^2\rangle$ and lies within the experimental error. Furthermore, the ratio of the slope of two different curves in the figure is determined by the inverse ratio of their deformation rates $\dot{\epsilon}$ as required by Eq. (26).

We also measured $R_D^{(\rho)}$ in ^{23}NaCl as a function of the slip plane orientation relative to the external field. No orientation dependence was observed within an error of about ±10%: This is in good agreement with the theoretical model used for the calculation of g_Q. So far only the qualitative agreement between theory and experiment has been discussed. In order to determine whether there is a quantitative agreement the values of the different parameters of Eq. (26), viz., A, $\langle\omega_D^2\rangle$ and $\langle\omega_Q^2\rangle$ should be known.

For the shape of the free induction decay after the locking pulse (see Fig. 5) the following expression is valid (Kanert and Mehring[22]):

$$S_n(t) = C_{-1/2}D(t) + C_S D(t)Q^+(t), \tag{33}$$

where $S_n(t)$ is the normalized decay function, $C_{-1/2}$ and C_S the transition probability coefficients and $D(t)$ and $Q^+(t)$ the dipolar and quadrupolar Fourier cosine transforms, respectively, of the distribution functions. With $I = \frac{3}{2}$ as for ^{23}NaCl one obtains[22]

$$C_{-1/2} = 0.366, \quad C_S = 0.634, \quad Q^+(t) = Q(2t).$$

Assuming Gaussian distribution functions

$$D(t) = \exp(-\tfrac{1}{2}\Delta^2 t^2) \tag{34}$$

and

$$Q(t) = \exp(-\tfrac{1}{2}\langle a^2\rangle t), \tag{35}$$

with $(\Delta^2)^{1/2}$ and $(\langle a^2\rangle)^{1/2} = \frac{1}{2}(\langle\omega_Q^2\rangle)^{1/2}$ (valid for $I=\frac{3}{2}$), the dipolar and quadrupolar linewidth, respectively, the resulting expression for $S_n(t)$ becomes

$$S_n(t) = 0.366\exp(-\tfrac{1}{2}\Delta^2 t^2) + 0.634\exp(-\tfrac{1}{2}\Delta^2 t^2)\exp(-2\langle a^2\rangle t^2). \quad (36)$$

From this analysis it was found that $\langle\omega_D^2\rangle \approx 32 \times 10^6$ sec^{-2}, in good agreement with the value of 40×10^6 sec^{-2} as given by Hebel.[28] Furthermore, the evaluation of the free induction decay shows that the root of the mean quadrupolar energy $\langle\omega_Q^2\rangle$ varies linearly with the applied stress for $\langle\omega_Q^2\rangle^{1/2}$ values of about $(1-7)\times10^3$ sec^{-1} as presented in Fig. 9. The diagram together with Eqs. (2) and (25) and $A = 0.13$ cm^2 sec^{-2} as given above confirms the well-known proportionality between the applied stress σ and $\sqrt{\rho}$. Evaluating the curve with $H_1 = 2$ G in Fig. 7, one obtains $R_D^{(\rho)} = 161\dot{\epsilon}$. Substituting these values in Eq. (26) it follows that $g_Q/n \approx 2.5 \times 10^{-4}$. From the calculated values of g_Q (Fig. 3) it is concluded that only dislocation jumps across large distances satisfy this equality.

In the case considered $g_Q \approx 1$ and $n \approx 4000$ Burgers vectors or $nb \approx 1.6\times10^{-4}$ cm. This agrees rather well with the distance between the dislocations given by $1/\sqrt{\rho}$ and which was found to vary between 5×10^{-4} cm and 0.5×10^{-4} cm in the deformation test (Fig. 9). This agreement would confirm the idea of dislocation motion impeded by forest dislocations. Because $R_D^{(\rho)}$ is a function of dislocation movement alone $R_D^{(\rho)}$ should be independent of temperature as long as the dislocation activation mechanism remains the same, which was confirmed by experiment.[4]

The values for $R_D^{(\rho)}$ for ^{23}NaCl and for ^{87}RbCl

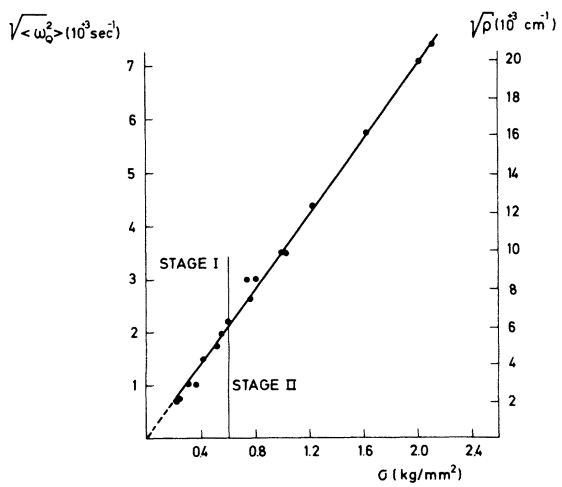

FIG. 9. Square root of the mean quadrupole energy $\langle\omega_Q^2\rangle$ and the total dislocation density ρ as functions of the applied stress σ. The well-known σ vs $\sqrt{\rho}$ law is experimentally confirmed.

(Fig. 7), where the same dislocation mechanism operates are different, since the factor $\langle\omega_Q^2\rangle / (\gamma^2 H_1^2 + \langle\omega_D^2\rangle + \langle\omega_Q^2\rangle)$ in Eq. (24) is different for both nuclei. For nuclei with spin I the mean quadrupolar energy $\langle\omega_Q^2\rangle$ can be written $\langle\omega_Q^2\rangle \simeq \text{const} \times q^2$ with $q = C_{11}Q$, where Q is the nuclear quadrupole moment and C_{11} is the corresponding matrix element of the gradient elastic tensor connecting the mechanical stress tensor linearly to the EFG tensor.[22] With the notation "1" for ^{87}RbCl, "2" for ^{23}NaCl, and $x = q(1)/q(2)$, the ratio $R_D^{(\rho)}(1)/R_D^{(\rho)}(2)$ of both the relaxation rates of the two systems (1, 2) measured in a rotating field of the same strength $H_1 = 2$ G is given by Eq. (24) as $R_D^{(\rho)}(1)$

$$\frac{R_D^{(\rho)}(1)}{R_D^{(\rho)}(2)} = x^2 \frac{\gamma^2(2)H_1^2 + \langle\omega_D^2(2)\rangle + \langle\omega_Q^2(2)\rangle}{\gamma^2(1)H_1^2 + \langle\omega_D^2(1)\rangle + x^2\langle\omega_Q^2(2)\rangle}.$$

The dipolar second moments and the gyromagnetic ratios γ of the two systems are nearly the same. Taking into account the different constants C_{11} and the different quadrupole moments (^{23}NaCl : $C_{11} = 7.5\times10^3$ dyn$^{-1/2}$,[22] $Q = 0.1$ b, ^{87}RbCl : $C_{11} = 32\times10^3$ dyn$^{-1/2}$,[29] $Q = 0.13$b (the value of C_{11} of ^{87}RbJ given in the paper is extrapolated to ^{87}RbCl taking into account the different shear modulus of both systems,[22] and using $\langle\omega_D^2(1)\rangle \approx \langle\omega_D^2(2)\rangle \approx 40\times10^6$ sec^{-2} together with $\langle\omega_Q^2(2)\rangle \approx 20\times10^6$ sec^{-2} (Fig. 9) for the ratio $R_D^{(\rho)}(1)/R_D^{(\rho)}(2)$ the value of approximately 8 is obtained. The latter is confirmed by the experiments (Fig. 7).

From the stress-time curves during stress relaxation the values of the strain rate sensitivity $(\partial\sigma/\partial\ln\dot{\epsilon})_{\epsilon,T}$ as a function of the mean value of σ were obtained (Fig. 10). This relationship is linear in accord with the well-known Cottrell-Stokes law. The occurence of this law together with the observed linear relationship between σ and $\sqrt{\rho}$ is usually interpreted as an indication that the mean free path of a dislocation is determined by the distance between the forest dislocations.[1]

VI. DISCUSSION

We have shown here that measurements of the nuclear relaxation time $T_{1\rho}$ in the rotating frame for ^{23}Na in NaCl and ^{87}Rb in RbCl single crystals as a function of deformation velocity furnish information on the mechanism of dislocation movement in solids.

In the present case where the mean quadrupolar energy does not exceed the mean dipolar energy the theories of Slichter and Ailion and of Rowland and Fradin can be adapted to correlate the mode of movement of dislocations with the nuclear relaxation rate. Furthermore an evaluation of the ^{23}Na free induction decays after the spin locking pulse leads to the mean quadrupole energy $\langle\omega_Q^2\rangle$ which is shown to be proportional to the applied

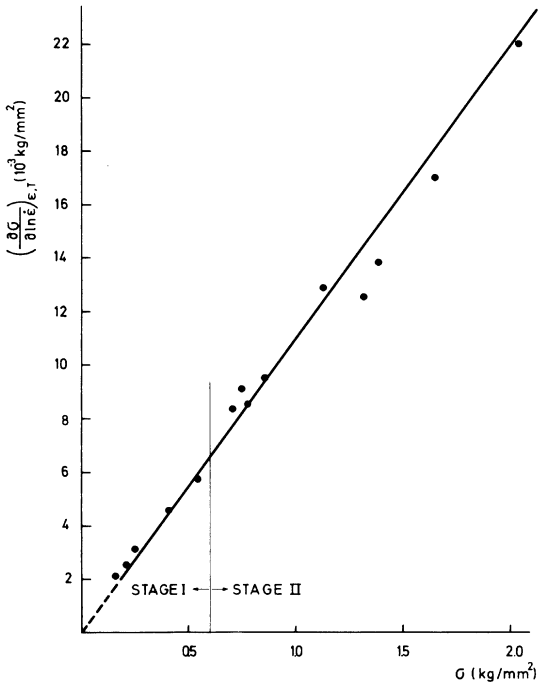

FIG. 10. Inverse strain-rate sensitivity as obtained from stress relaxation experiments vs the mean value of σ during stress relaxation. The experimental data confirm the Cottrell-Stokes law.

stress, i.e., the well-known σ-$\sqrt{\rho}$ law is valid.

It is well known that during plastic deformation point defects as well as dislocations are produced, and NaCl is no exception to this, as is obvious from the experimental evidence of Davidge and Pratt.[13] The density of these point defects increase with increasing strain. If the relaxation rate $R_D^{(\rho)}$ would be due to these point defects, one would expect it to be a function of ϵ; within the limits of accuracy of the experiment, this is not observed. It would seem safe to conclude that $R_D^{(\rho)}$ contains no significant contribution from point defect movement.

So far our results and the usual solid-state theories are consistent. Not quite clear at the moment however is the variation of the dislocation mean free path with strain: from Eq. (26) together with the data presented in Fig. 7 it would follow that with increasing strain $\langle\omega_Q^2\rangle$ increases and therefore n decreases. This decrease is not as large as would be expected from the decrease in distance between dislocations with strain from Fig. 9.

Comparing the results from the nuclear relaxation experiments to those obtained from strain rate sensitivity measurements the fact has to be noted that the first method gives the mean distance covered by a unit activated dislocation segment whereas the second method gives the mean distance covered by an activated dislocation segment which has, by the assumed random distribution of obstacles, the same length as this distance. Combining the results of the nuclear relaxation experiments and the strain rate sensitivity measurements we arrive at the interpretation that both in stage I and stage II decreasing lengths of the dislocation lines are activated to move over a more or less constant distance with increasing strain.

Consider the findings of Heidemann[12] and Hesse[11]: during pre-yield slip and also dislocation multiplication has taken place on all four slip systems. Heidemann observed that the dislocation density in a plane in which slip takes place is saturated. After approximately 0.2% of plastic deformation the distance between the dislocations in the slip plane reaches a minimum value of approximately 1.2×10^{-4} cm.

The number of the slip planes activated increases with increasing strain mainly by multiple cross slip out of the original slip planes. Thus broadening slip bands form, which eventually fill the crystal at the end of stage I. The distance between the slip bands then is of the order of the distance between the dislocations in the slip planes. The polygon walls formed early in stage-II limit the propagation of the activated dislocation segments in the direction of the Burgers vector. The distance between these walls—1.2×10^{-4} cm—agrees well with the mean distance covered by a unit activated dislocation segment—1.6×10^{-4} cm.

It must be emphasized, however, that this interpretation is necessarily highly speculative at this stage. In order to obtain a more detailed insight in the dislocation processes taking place during plastic deformation in NaCl various other nuclear relaxation experiments should be carried out on (i) crystals compressed along $\langle110\rangle$; (ii) crystals doped with impurities or irradiated before deformation with neutrons which would limit the mean free path of the dislocations.

Initial results of new measurements (Hackelöer[30]) indicate that it should be possible to extend this work to higher deformation rates and to systems where $\langle\omega_Q^2\rangle$ is noticeable larger than $\langle\omega_D^2\rangle$. For such cases the SARF model ceases to be valid and one has to apply a more general theory as given by Wolf.[31]

ACKNOWLEDGMENTS

The authors wish to thank Professor M. Mehring for his stimulating discussions of this work. This study was performed as part of a project on the investigation of dislocation dynamics jointly sponsored by the Foundation for the Research on Matter, F. O. M. and the Metaalinstituut T. N. O. at Apeldoorn. Financial support by the "Herbert-Quandt-Stiftung" is gratefully acknowledged.

[1]D. Klahn, A. K. Mukherjee, and J. E. Dorn, in Proceedings of the Second International Conference on the Strength of Metals and Alloys (American Society for Metals, Ohio, 1970), Vol. III, pp. 951 ff.
[2]J. J. Gilman, Micromechanics of Flow in Solids (McGraw-Hill, New York, 1969), pp. 157 ff.
[3]W. G. Johnston, and J. J. Gilman, J. Appl. Phys. 30, 129 (1959).
[4]G. Hut, A. W. Sleeswyk, H. J. Hackelöer, H. Selbach, and O. Kanert, Solid State Commun 15, 1115 (1974).
[5]G. Hut, H. J. Hackelöer, H. Selbach, O. Kanert, and A. W. Sleeswyk, *Proceedings of the 18th Congress Ampere, Nottingham, 1974* (North-Holland, Amsterdam, 1975).
[6]G. Hut, A. W. Sleeswyk, H. J. Hackelöer, H. Selbach, and O. Kanert, Solid State Commun. 17, 85 (1975).
[7]C. P. Slichter, and D. Ailion, Phys. Rev. 135, A 1099 (1964).
[8]T. J. Rowland, and F. Y. Fradin, Phys. Rev. 182, 760 (1969).
[9]P. L. Pratt, Acta Metall 1, 103 (1953).
[10]S. J. Mendelson, Appl. Phys. 33, 2175 (1962).
[11]J. Hesse, Phys. Status Solidi 9, 209 (1965).
[12]K. F. Heidemann, thesis University of Münster, 1973 (unpublished).
[13]R. W. Davidge, and P. L. Pratt, Phys. Status Solidi 6, 759 (1964).
[14]A. S. Argon, A. G. Nigam, and G. E. Padawer, Philos. Mag. 25, 1095 (1972).
[15]J. Hesse, and L. W. Hobbs, Phys. Status Solidi 14, 599 (1972).
[16]J. Hesse and K. H. Matucha, Scr. Metall 6, 865 (1972).
[17]K. H. Matucha, Phys. Status Solidi 26, 291 (1968).
[18]K. H. Matucha, W. Franzbecker, and M. Wilkens, Phys. Status Solidi 33, 493 (1969).
[19]A. J. E. Foreman and M. J. Makin, Philos. Mag. 20, 911 (1966).
[20]A. Abragam, The Principles of Nuclear Magnetism, (Oxford, University, London, 1973), pp. 560 ff.
[21]T. C. Farrar, and E. D. Becker, Pulse and Fourier Transform NMR (Academic, New York, 1971), p. 91 ff.
[22]O. Kanert, and M. Mehring, *Static Quadrupole Effects in Disordered Cubic Solids* (Springer-Verlag, Berlin, (1971), Vol. 3, pp. 62 ff.
[23]W. Baumhoer, J. Thiemann, and O. Kanert, Phys. Status Solidi 73, (1976).
[24]F. W. De Wette, Phys. Rev. 123, 103 (1961).
[25]F. W. De Wette, and G. E. Schacher, Phys. Rev. 137, A92 (1965).
[26]F. Granzer, G. Wagner, and J. Eisenblätter, Phys. Status Solidi 30, 587 (1968).
[27]J. S. Waugh, *Advances in Magnetic Resonance* (Academic, New York, 1971), Vol. V, pp. 147 ff.
[28]L. C. Hebel, Solid State Phys. 15, 457 (1963).
[29]H. J. Hackelöer, and O. Kanert, J. Magn. Reso. 17, 367 (1975).
[30]H. J. Hackelöer, thesis (University of Dortmund, 1976) (unpublished).
[31]D. Wolf, Phys. Rev. (to be published).